ISSN 0024-4902, Lithology and Mineral Resources, 2019, Vol. 54, No. 4, pp. 273–291. © Pleiades Publishing, Inc., 2019.
Russian Text © The Author(s), 2019, published in Litologiya i Poleznye Iskopaemye, 2019, No. 4.

Glauconite in the Lower Cambrian Terrigenous–Carbonate Rocks, Olenek Uplift, North Siberia

T. A. Ivanovskaya[a, *], A. R. Geptner[a], A. T. Savichev[a], T. S. Zaitseva[b], N. V. Gor'kova[a], and E. V. Pokrovskaya[a]

[a] *Geological Institute, Russian Academy of Sciences, Pyzhevskii per. 7, Moscow, 119017 Russia*

[b] *Institute of Precambrian Geology and Geochronology, Russian Academy of Sciences, nab. Makarova 2, St. Petersburg, 199034 Russia*

**e-mail: tat.ivanovsckaya2012@yandex.ru*

Received October 29, 2018; revised November 6, 2018; accepted November 14, 2018

Abstract—This work considers for the first time mineralogical features of the Lower Cambrian (Tommotian) glauconite collected from terrigenous–carbonate rocks of the Kessyusa Group (upper part of the Mattaia Formation and lower part of the Chuskuna Formation), as well as from basal beds of the overlying limestones of the Erkeket Formation. Samples were taken from three sections on the northwestern slope of the Olenek Uplift, North Siberia. Their stratigraphic assignment is given on the basis of recent data (Nagovitsin et al., 2015 and others). Grains of the layer silicates are made up of the mixed layer mica–smectite phases with relatively low (<10%) and higher (10–20%) contents of expandable layers (unit cell parameter $b = 9.06–9.12$ Å). Micaceous minerals form a series from glauconite to Al-glauconite (Al index $K_{Al} = {}^{VI}Al/({}^{VI}Fe^{3+} + {}^{VI}Al)$ is 0.11–0.47 and 0.60, respectively), with the K_2O content varying from 6.80 to 8.54%. Detailed lithological-mineralogical characteristics is given for the first time for the glauconite-bearing rocks, the primary sediments of which were accumulated in the prefrontal beach zone and transitional beach–shelf zone in the Siberian epicontinental marine paleobasin (Marusin, 2016). Origin of the studied grains (authigenic, allothigenic) is discussed and their secondary alterations at different stages of lithogenesis are considered (rewashing, phosphatization, pyritization, calcitization, ferrugination, and others). It is shown that the obtained preliminary Rb–Sr dates (450–320 Ma) are "rejuvenated" and do not correspond to the age value of 541.0 Ma accepted for the Vendian–Lower Cambrian boundary (Gradstein et al., 2012). This can be related to diverse secondary alterations of the glauconite grains during the rewashing, transportation, and different stages of diagenesis of primary sediments after their redeposition, as well as at stages of catagenesis and hypergenesis of the glauconite-bearing rocks.

DOI: 10.1134/S0024490219040035

INTRODUCTION

This work is aimed at studying the mineralogical, structural, and crystal-chemical (including Mossbauer) features of the globular layer silicates of the glauconite–illite series from the upper part of the Lower Cambrian Kessyusa Group (Olenek Uplift). This investigation was accompanied by analyzing the lithological–mineralogical composition of host rocks. The obtained data provided insight into the genesis of glauconite grains (authigenic grains formed in situ and allothigenic rewashed grains), as well as their secondary transformations. Detailed study of the glauconite–illite minerals is required to carry out isotope-geochronological studies, which were preliminarily performed for samples from the Chuskuna and Erkeket formations. The detailed Mossbauer and isotope-geochronological data will be considered in the next communication.

Glauconites are usually characterized by the globular shape and ascribed to the dioctahedral micaceous minerals with high Fe^{3+} content. Owing to the isovalent Fe^{3+}–Al substitutions in octahedra, the micaceous minerals define a series from glauconite through Al-glauconite and Fe-illite to illite, as shown in (Kossovskaya and Drits, 1971; Drits and Kossovskaya, 1991; Drits et al., 2013; Ivanovskaya et al., 2012, 2015, 2017a, 2017b; Zviagina et al., 2017, and others).

The problem of glauconite genesis consists of many questions that remain ambiguous. Among these questions, of particular interest is the position of glauconite formation in the multistage evolution of lithogenesis. It was noted that globules could be formed during sedimentation, diagenesis, or through a multistage sedimentation–diagenetic process. We accepted in this paper that glauconite is formed through the diagenetic transformation of a sediment from the iron–silica gel, which, according to V.I. Vernadskii, is formed during

Fig. 1. Geographic position of the studied sections on the Khorbusuonka (1) and Olenek (2) rivers and in the Debengde River basin, upper reaches of the Khary-Yallakh River (3).

the metabolic bacterial activity (Drits et al., 1993; Geptner and Ivanovskaya, 1998, and others).

As known, glauconite sediments frequently bear traces of the mixing, stirring, and rewashing, which could be related both to bioturbation and change of hydrodynamic conditions during sedimentation. This is also the case with the studied sediments, which contain the allothigenic and authigenic grains. There are no generally accepted criteria for their distinction. We encountered this problem during study of the Lower Cambrian sequences.

STUDY OBJECTS

The history of study of the Vendian–Cambrian boundary sediments of the Olenek Uplift and, in particular, the Kessyusa Formation, is described in detail in (Marusin, 2016). Note only that the Kessyusa Formation (Group), the most representative sections of which are exposed in the Olenek and Khorbusuonka river basins, is represented by terrigenous–carbonate sediments, with stratiform bodies of volcanogenic conglobreccias in the lower parts of some sections. The formation rests with a hiatus on dolomites of the Turkut formation of the Vendian Khorbusuonka Group and is overlain with erosion by the red-colored limestones of the Lower Cambrian Erkeket Formation.

Some researchers recently proposed to transfer the Kessyusa Formation to the Kessyusa Group and subdivide it into three formations: Syargalakh, Mattaia, and Chuskuna (Rogov et al., 2015; Nagovitsin et al., 2015; Marusin, 2016). The Mattaia Formation 92 m thick is mainly made up of terrigenous rocks, while the Chuskuna Formation (26.5 m) is mainly represented by wavy bedded sandstones, and, most importantly, includes the previously unexposed and unstudied upper part of the Kessyusa Group consisting of horizontally bedded sandstones, mudstones, and siltstones. This part of the formation is recovered by trenches and ditches (Olenek River, upper reaches of the Kersyuke River). Based on paleontological data, the upper part of the Mattaia Formation and Chuskuna Formation are ascribed to the Lower Cambrian Tommotian Stage (zone *N. sunnaginicus*), while the underlying part of the Kessyusa Group belongs to the Upper Vendian Nemakit–Daldynian Stage (Rogov et al., 2015; Nagovitsin et al., 2015; Marusin, 2016, and others). In this work, the stratigraphic assignment of samples is given on the basis of these modern data.

It was noted for the first time in (Nagovitsin et al., 2015) that the northeastern sections of the Olenek Uplift and, in particular, the section on the right bank of the Khorbusuonka River (in front of the Mattaia River mouth) include only the lower part of the Chuskuna Formation (~12 m), while the upper 15 m is eroded. The authors studied glauconite in front of the Mattaia River mouth, where it was sampled by Ivanovskaya in 2000 (Fig. 1). In this section, we studied the upper parts of the Mattaia Formation and the lower part of the Chuskuna Formation (~12 m), as well as the overlying limestones of the Erkeket Formation (Fig. 2a).

Thus, the studied samples were collected: (1) on the right bank of the Khorbusuonka River (in front of the Mattaia River), 0.1–0.2 m above the base of the Erkeket Formation (samples 592, 592A), from conglomerate lenses at the Chuskuna–Erkeket formations boundary (sample 593), as well as from the upper part of the Mattaia Formation (samples 599, 599A, 599B, 1175/32), where sample 1175/32 was taken by G.V. Krutii (Cosmoaerogeological Expedition (KAGE) no. 3) and from the lower part of the Chuskuna Formation (samples 594–598, 599C, 599D, 603, 604); (2) on the Olenek River (in front of

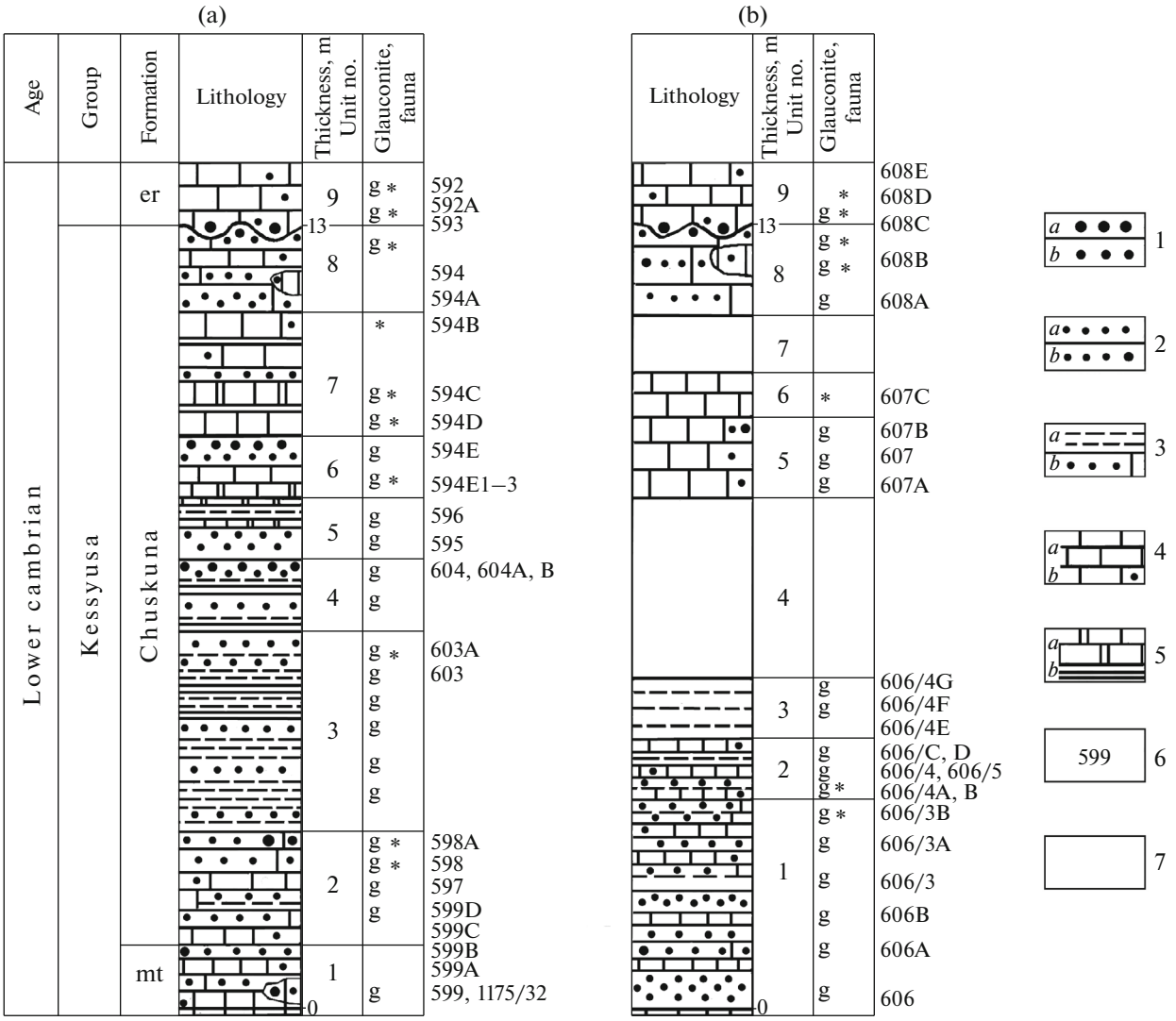

Fig. 2. Schematic sections of the upper part of the Kessyusa Group and the roof of the Erkeket Formation on the Khorbusuonka (a) and Olenek (b) rivers. Formations: (mt) Mattaia, (er) Erkeket. (1) Conglomerates (a), gravelstones (b); (2) sandstones (a), gravelly sandstones (b); (3) siltstones (a), sandstones (calcic and calcareous) (b); (4) limestones (a), sandy limestones (b); (5) limestones and dolomites (a), mudstones (b); (6) sample number; (7) grass-covered.

the Suordakh River mouth), 0.1–0.5 m above the base of the Erkeket Formation (samples 608D, 608E), from boundary sediments of the Erkeket and Chuskuna formations (sample 608C), and from the Chuskuna Formation (samples 606–608A, 608B; Fig. 2b); and (3) in upper reaches of the Khary–Yallakh River (right tributary of the Kyutingde River, Olenek River basin) from the base of the Erkeket Formation (sample 1783 kindly given by geologists A.G. Kats and Z.B. Frolova (KAGE no. 3) (Fig. 1).

Glauconite was previously found at different stratigraphic levels of the Kessyusa Group (Formation) and in lower parts of the Erkeket Formation by many researchers (Missarzhevskii, 1980, 1982, 1989; Vodanyuk and Karlova, 1988; Karlova and Vodanyuk, 1985; Knoll et al., 1995; Marusin, 2016; and others), but was not studied in detail. Glauconite-bearing rocks most suitable for the extraction of grains for the detailed study were found by Ivanovskaya in the first and second sections.

It should also be noted that the studied rocks contain numerous rounded and oval concentrically zoned calcite segregations, which are termed by different authors as ooliths and ooids (chemogenic), as well as oncoliths (oncoids), which are regarded as products of the algal activity. Authors who studied the considered Lower Cambrian sediments with similar segregations term them ooliths (Vodanyuk and Karlova, 1988; Karlova and Vodanyuk, 1985; Knoll et al., 1995; Nagovitsin et al., 2015; Marusin, 2016; and others) and (or) oncoliths (Missarzhevskii, 1980; and others). In this work, such segregations are termed “ooliths,” because

confirmation of their algal nature is beyond the scope of this study. It should only be noted that one of the authors (A.R. Geptner) ascribes them to oncoliths.

Lithological description of units distinguished in the first and second sections (from the bottom to top) (Figs. 2a, 2b) and characteristics of sample from the Erkeket Formation (section 3) are given below.

First Section, Khorbusuonka River

1. *Mattaia Formation*. Greenish gray glauconite sandstones and detrital–oolithic limestones. The sandstones are inequigranular, locally gravelly and calcareous (samples 599, 599A, 1175/32). The rocks are massive and bedded. The bedding is frequently emphasized by numerous grains of mafic minerals, which also can be randomly distributed. Samples were taken from the unit base: from detrital–oolithic limestones (sample 599) and limestone lens with gravel- and sand-size glauconite grains. These grains are rounded and semirounded fragments of almost completely glauconitized limestone (calcite ~26%) with phosphate admixture (8%) (sample 1175/32). Thickness 1 m.

2–8. *Chuskuna Formation*.

2. Alternation of massive coarse-grained sandstones (up to gravelstones) and variably clayey and calcareous, finer-grained siltstones and sandstones (samples 597, 598, 598A, 599B–599D) with rare interbeds of clastic–oolithic limestones. Bedding is horizontal and cross. As the first unit, this unit contains mafic minerals. The roof of gravelly sandstones contains ooliths and separate large pebbles (sample 598A). Glauconite (sample 598) was taken from the underlying inequigranular calcareous sandstones with fragments of ooliths, large pebble, and small gravel, as well as from the detrital–oolithic limestones. Thickness ~2 m.

3. Thin alternation of siltstones and fine- to medium-grained sandstones with thin clayey intercalations. Sandy–silty light and greenish gray, variably glauconitized, clayey, and (or) calcareous, as well as dolomitic rocks. The rocks show wavy, cross, and horizontal (thin-, micro-) bedding with fine pyrite grains and numerous small grains of mafic minerals, which frequently emphasize the bedding (samples 603, 603A). Mudstones are bluish gray and strongly weathered. Thickness 3–3.2 m.

4. Massive pinkish gray, locally strongly weathered gravelstones, and greenish gray coarse- and fine-grained sandstones with thin intercalations of dark gray mudstones and siltstones. Bedding is horizontal and emphasized frequently by well-preserved glauconite grains and more rarely cross bedding (samples 604, 604A, 604B). Glauconite is ubiquitously developed. Thickness 1.2 m.

5. Glauconite (inequigranular coarse- to fine-grained, locally silty) sandstones (sample 595). They are overlain by light and dark gray thin- to micro-bedded siltstones with admixture of carbonates, alternating with silty carbonates (calcite, dolomite), with glauconite grains (sample 596) along bedding planes. Thickness 1 m.

6. Brownish gray and gray fine-grained limestones with quartz admixture and layerwise distribution of glauconite, oolith, scarce fragments of shells, and fine-grained dolomite (sample 594E1–3). Upsection, they grade into the pinkish gray coarse-grained sandstones and gravelstones with small glauconite (≤0.1 mm) grains (sample 594E). Thickness 1 m.

7. Fine to micrograined (micritic) and fine-grained limestones containing fine-shelly fauna and ooliths with thin rare intercalations of dolomites, as well as greenish gray fine-grained and inequigranular glauconite sandstones and mudstones. Thin (to micro) wavy and horizontal bedding (layers up to 2–5 mm thick) (samples 594B–594D). Thickness 2 m.

8. Greenish gray, inequigranular, locally gravelly and calcareous sandstones with intercalations and lenses of oolithic sandy–silty limestones. Glauconite is ubiquitously developed in the rocks. Hematite and secondary calcite are developed in some places along rough bedding planes with erosion traces emphasized by the strongly weathered glauconite rock. The rocks show horizontal, wavy, lenticular, and cross bedding. There are scarce fragments of shells and thin layers of mafic minerals (samples 594, 594A). Glauconite sample was taken in the upper part of the unit from the detrital–oolithic limestone and inequigranular calcareous sandstone (sample 594). Thickness 1.5 m. Total thickness of units 1–8 is ~13 m.

9. *Erkeket Formation*. The uneven (with pockets) surface of the above-described gray-colored rocks of the Chuskuna Formation is overlain by brick-red, more rarely greenish gray, limestones. The pockets are filled with calcareous conglomerates (pebbles up to 3 or 4 cm) (sample 593) overlain by thin-platy clayey limestones (sample 592A) (glauconite sample 592 was taken above the latter interval). The limestones are inequigranular (from micritic to fine-grained), with rough bedding planes, mud eater tracks, and numerous organic remains. Thickness of the studied part of the formation is ~2 m.

Second Section, Olenek River

1–8. *Chuskuna Formation*.

1. Siltstones and fine-grained sandstones with intercalations of variably glauconitic, locally ferruginated oolithic sandy–silty limestones. The siltstones and sandstones have mainly thin (cross, horizontal) bedding, which is frequently emphasized by fine grains of mafic minerals (samples 606/3, 606/3A, 606/3B). The lower part of the unit is made up of massive, coarse-grained, locally gravelly sandstones interca-

lated with detrital–oolithic limestones (samples 606, 606A, 606B). Thickness 3.2–3.5 m.

2. Alternation of light greenish gray and dark gray glauconite sandstones, siltstones, and oolithic limestones. The rocks are thin-bedded, with intercalations of mafic grains (samples 606/4, 606/5, 606/4A–606/4D). Glauconite samples were taken along the strike, 10 m from each other, from interbeds of detrital–oolithic limestones and sandstones (samples 606/4, 606/5). Thickness 1 m.

3. Platy (1–3 cm) thin-bedded intensely clayey siltstones, locally with glauconite. The rocks show horizontal, cross and wavy bedding (layer thickness from 6–5 mm to <1 mm). There are traces of sediment stirring and worm trails (sample 606/4E–606/4G). Thickness 1 m.

4. Grass-covered. Thickness around 3 m.

5. Dense, glauconitic, detrital-oolithic limestones forming a clear ledge in the topography, with lenticular-wavy and wavy bedding (samples 607, 607A, 607B). Glauconite sample was taken ~0.5 m from the unit base (sample 607). Thickness 1.5 m.

6. Intensely weathered limestone with numerous accumulations of fine-shelly fauna. The rock is pinkish and gray-green, variegated, with insignificant amount of glauconite (sample 607C). Thickness 0.7 m.

7. Grass-covered. Thickness about 1 m.

8. Calcareous, locally gravelly, inequigranular sandstone with lenses and intercalations of oolithic limestone. The rocks form a clear ledge in topography. They are light and yellowish gray with greenish tint and glauconite grains, rarely ferruginated (samples 608A–608C). Sample 608C was taken from boundary layers of the described sandstones and the overlying Erkeket limestones. Flat-pebbled conglomerates similar to those on the Khorbusuonka River were found in pockets at the contact of sandstones and limestones. Thickness about 1.5 m. Total thickness of units 1–8 ~13 m.

9. *Erkeket Formation*. Rocks of the formation are similar to those described in the Khorbusuonka River basin. Brick-brown and greenish gray glauconite-bearing limestones (sample 608D). The pale green clayey limestone (sample 608E) was studied 0.5 m above the boundary. Thickness 2 m.

Third Section, Debengda River Basin

Brick-brown and greenish gray glauconite-bearing organogenic limestones from the base of the Erkeket Formation, upper reaches of the Khary-Yallakh River (Fig. 1, point 3), similar to the above-described rocks on the Khorbusuonka and Olenek rivers (sample 1783).

METHODS

Glauconite-bearing rocks were studied using optical methods and scanning electron microscopy (SEM) coupled with microprobe and X-ray analysis including the study of separate minerals (Fe-rich, carbonate, clayey, and others). Glauconite grains were studied by the same methods, as well as using chemical and microprobe analyses, Mossbauer spectroscopy, and isotope-geochronological analyses. The methods are described in (Ivanovskaya et al., 2012; Zaitseva et al., 2016, 2018). Depending on the amount of material, the samples were studied in variable detail.

Glauconite grains were extracted from rocks using the conventional technique (Ivanovskaya et al., 2012). Size fractions in five samples (samples 592, 595, 1175/32, 607, 1783) were separated using a heavy liquid density column, with a subsequent ultrasound treatment. Note also that the grains of layered silicates in samples 594E1, 596, 608C, 606/4, and 606/3A were studied together with host rock only in thin (petrographic and polished) sections.

Complete silicate microanalysis was obtained for samples 1175/32, 607, and 1783 (analyst K.A. Stepanova), while the quantitative cation analysis was carried out using microprobe studies of separate grains from sample 595 on an X-ray Camebax microprobe (analyst G.V. Karpova). The study of glauconite microstructure in polished thin sections, separate grains, and host rock areas, as well as the semiquantitative cation analysis of glauconite grains and surrounding minerals were carried out using a CamScan MV-2300 SEM equipped with EDS INCA-200 (Oxford-Instrument) (samples 592, 594, 594D, 594E1, 596, 595, 598, 599, 1175/32, 608C, 607, 606/4, 606/5, and 606/3A). Microanalysis was carried out in a point 1 μm^2 in area.

Proportions of the di- and trivalent Fe cations of in 2 : 1 sheets of dioctahedral layer silicates were specified using the Mossbauer spectroscopy for samples 1783 (Erkeket Formation), as well as for samples 595, 1175/32, and 607 (Chuskuna Formation). For the remaining ten samples mentioned above, the proportions were taken arbitrarily. For sample 592 (Erkeket Formation), the proportion was taken to be the same as in sample 1783 from the Erkeket Formation (0.12). For samples from the first and second sections of the Chuskuna Formation, the proportions were calculated using the data obtained for samples 595 and 607 from the same formation (0.17 and 0.26, respectively).

RESULTS

General Characteristics of Rocks

In two sections of the Mattaia and Chuskuna formations (about 13 m thick) spaced 36 km apart from each other, glauconite occurs in terrigenous sediments, gray-colored limestones, and their transitional varieties, as well as in scarce intercalations of dolomitized limestones (Figs. 3–5). The glauconite-bearing rocks are mainly represented by brick-brown detrital limestones in the Erkeket Formation and by calcar-

eous conglomerates of the same color at the contact with the Chuskuna Formation. The X-ray and microprobe studies of rocks allowed us to specify their mineral composition (Table 1). We shall consider briefly their features.

Limestones. The rocks usually contain glauconite grains, films of organic matter (OM), sandy–silty admixture of quartz (5–50%) and less common feldspars, ooliths, as well as fragments of shells, ore and clay minerals, and other minerals at some levels (Figs. 3, 4a–4d). They are mainly made up of the micritic (micro- to fine-crystalline), fine-crystalline and holocrystalline calcite.

Inequigranular calcite (from coarse- to micrograined) replaces glauconite, oolith, and terrigenous grains to a variable extent. In the first (units 1, 6–8) and second (1, 2, 5, 6, 8) sections, glauconites of diverse (including globular) shape and their relicts occur within ooliths. In the second section (unit 5), we studied in detail grains extracted from ooliths and host limestone (sample 607) (Figs. 2, 4a, 4b).

The calcareous conglomerates fill pockets at the boundary of the Chuskuna and Erkeket formations (samples 593, 608C). Pebbles (from 1–4 to 15 cm in size) are mainly represented by the varicolored (light and dark gray, pinkish brown, yellowish, and others) micro- to fine-crystalline limestones frequently with inclusions of large quartz and glauconite grains, as well as ooliths. Sometimes, the conglomerates contain pebbles of the underlying rocks. The conglomerate cement consists of inequigranular limestones and calcareous-gravelly quartz sandstones with ooliths and grains of glauconite of different size.

Microprobe data showed that calcite from the groundmass and cement in detrital limestones, as well as ooliths, are virtually devoid of isomorphic admixtures, while dolomites are mainly represented by the Fe-rich (more rarely, Fe–Mn) varieties. Pure dolomite is scarce (Table 1).

Dolomites and Fe-dolomites. The dolomites were found only in limestones of the Erkeket Formation, where they compose intricate angular fragments replaced by calcite in margins (samples 592A, 592) (Table 1, Fig. 5f). The fine-grained Fe-dolomite as minor admixture (up to traces) was found at different stratigraphic levels in both sections. The mineral predominates in separate carbonate intercalations of the Chuskuna Formation, where calcite either occurs as insignificant admixture (samples 594E3, 596) or is intercalated with Fe-dolomite (sample 594C) (Table 1, Fig. 5h). The Fe-dolomite in these rocks can be neutral with respect to glauconite grains or almost completely replaces the latter mineral (Figs. 4e, 4f). The coarse- to medium-grained Fe-dolomite is observed in limestones as separate aggregates or replaces calcite ooliths and other mineral segregations (samples 608C, 607, 594, 594C, and others) (Fig. 5b).

Calcite, dolomite, and Fe-dolomite were determined on the basis of several main reflections, which are typical of these minerals and recorded in the X-ray powder diffraction (XRD) patterns of unoriented samples (3.85, ~3.03, 2.28, 2.094, 1.91, 1.87 Å; 2.885, 2.192, 1.79 Å, and 2.903–2.917, 2.206, 1.801 Å, respectively). While analyzing the XRD patterns of the unoriented samples, the main attention was focused on the values of interplanar spacing *d* (104). The most intense peak of dolomite in the studied samples is characterized by 2.88–2.89 Å, while reflections in dolomites with high Fe (FeO = 3.93–14.52%) and sometimes Mn (MnO = 0.59–4.44%) contents vary from 2.903 to 2.917 Å. Such rocks are ascribed to Fe-dolomites (Vasil'eva and Vasil'ev, 1980; Rolli et al., 1996).

Thus, the studied carbonate rocks with variable content of terrigenous admixture are mostly made up of the detrital–oolithic limestones with glauconite, while the detrital and clayey limestones, as well as calcareous conglomerates with glauconite are less common. Dolomitized limestones are occasional.

Terrigenous rocks. Terrigenous rocks are represented by gravelstones (samples 594E, 604), as well as coarse-grained (sample 606A), inequigranular (from coarse- to fine-grained) (samples 594, 595, 599B, 608C, and others), and fine-grained (samples 597, 604A, 606/3A, and others) sandstones. The sandstones (coarse and inequigranular) can be variably enriched in gravel (2–10 mm) and sometimes also contain separate large (up to 12 cm long) pebbles of limestones and fine-grained sandstones (sample 598A). Both sections also contain siltstones: second to fourth units in the first section and first to third units in the second section (Figs. 2, 4h, 5h, Table 1).

The rocks are quartz and feldspar–quartz in composition, with admixture of calcite (5–50%), sometimes clayey, variably glauconitized, with rare flakes of biotite and muscovite. They sometimes contain ooliths (samples 594, 606/3A), semirounded and rounded grains of oolithic limestones, phosphates, and cherts, as well as ore minerals. The cement is made up of glauconite, carbonate (calcite, Fe-dolomite), finely dispersed layer silicates (mica and (or) chlorite), and Fe-rich minerals (pore, basal, and film types). Authigenic quartz occurs in the cement of only sandstones of the first section (samples 604A, 595). These rocks have mainly conformal–regeneration textures. In other samples, such textures are rare, because the carbonate and (or) clayey cement is widespread. The coarse-grained carbonate (calcite, Fe-dolomite) forms the pore and basal cement, which is most developed in the interbeds of gravelstones and coarse-grained inequigranular sandstones, sometimes with gravel admixture (samples 604, 604B, 599B, 606A).

The main types of terrigenous rocks are gravelstones and gravelly sandstones with the calcareous admixture, calcareous glauconitic sandstones with the

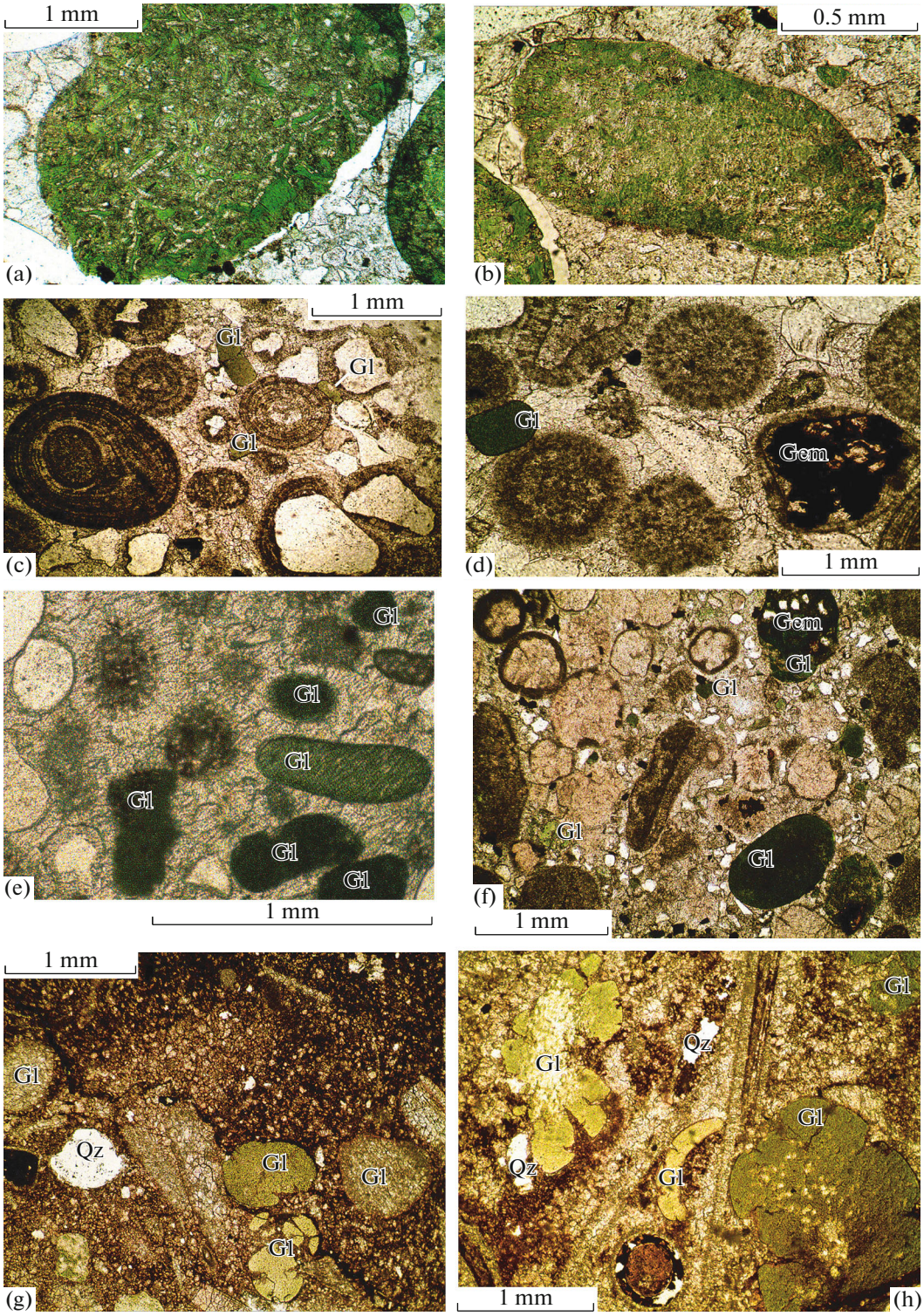

Fig. 3. Glauconite grains in limestones of the Mattaia (a–b), Chuskuna (c, f), and Erkeket (g, h) formations. Photomicrographs of polished thin sections. Parallel nicols. (a, b) Rounded grains of gravel- and sand-size glauconite in a limestone lens (sample 1175/32); (c, d) detrital–oolithic limestone with sandy–silty admixture and glauconite (sample 599); (e) detrital–oolithic limestone with green and dark green glauconite grains of irregular and globular shape (sample 594); (f) detrital–oolithic limestone with large dark green globule; in the upper part of the polished thin section, glauconite is almost completely replaced by hematite; ooliths are variably recrystallized (sample 606/4a); (g, h) detrital limestones with glauconite globules of cerebriform and rounded shape and green color of variable intensity and tints (samples 592 and 608C, respectively) (sample 608C contains glauconitized shell valve). (Gl) glauconite, (Qz) quartz, (Hem) hematite (hereinafter).

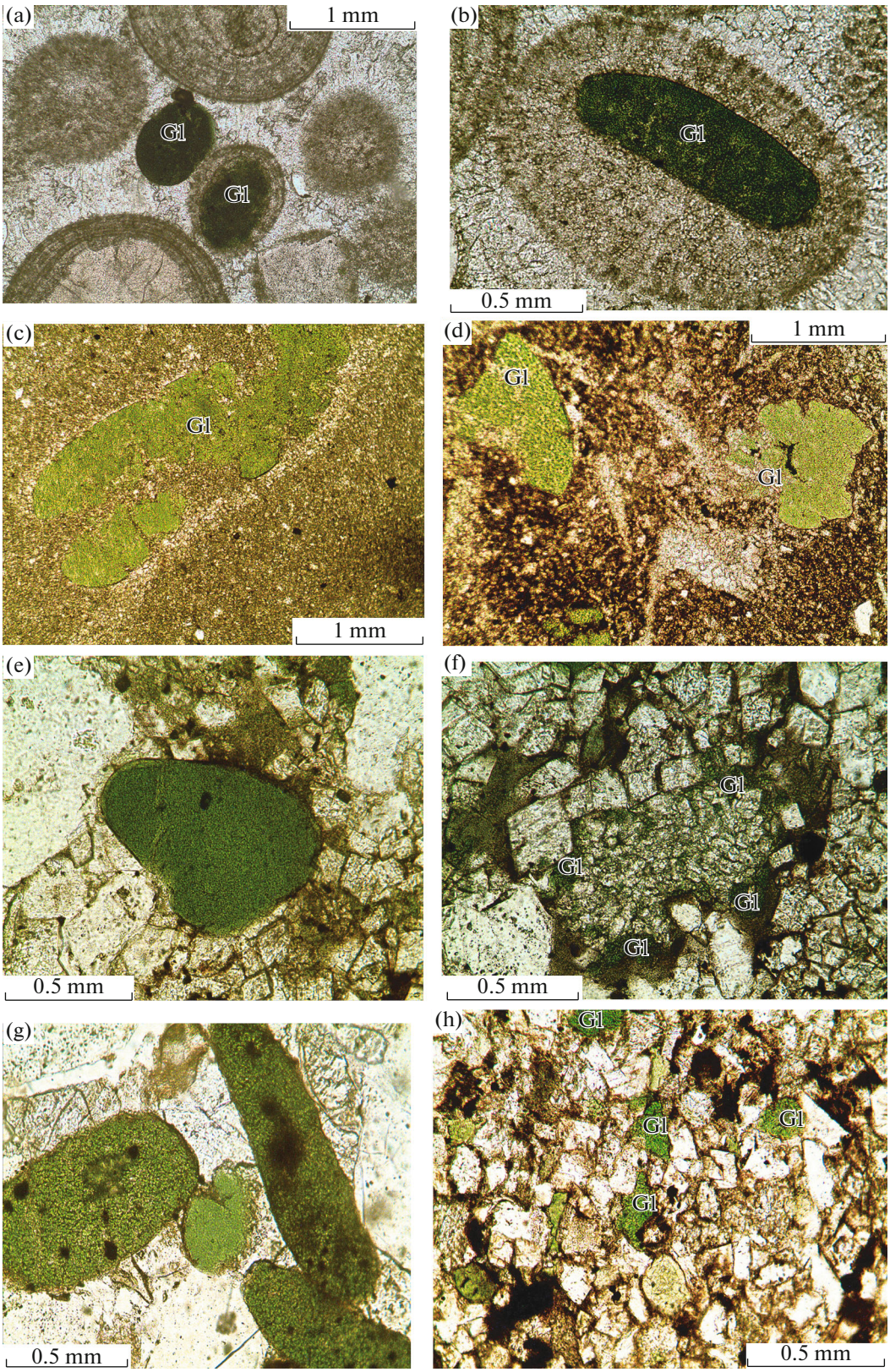

Fig. 4. Glauconite grains in the terrigenous–carbonate rocks of the Chuskuna (samples 607, 594C, 595, 596) (a, b, e–h) and Erkeket (sample 1783) (c, d) formations. Photomicrographs of polished thin sections. Parallel nicols. (a, b) Glauconite globules in oncoliths and host limestone (sample 607); (c, d) brick-red detrital limestones with glauconite grains of different size, shape, and degree of preservation (sample 1783); (e, f) in Fe-dolomite interbeds, glauconite grain with neutral contacts (e) and almost completely replaced by this mineral (f) (sample 594C); (g) inequigranular quartz sandstone with mosaic texture (sample 595) with glauconite grains of green color of different intensity (dark inclusions inside are hematite); (h) quartz siltstone with glauconite (sample 596).

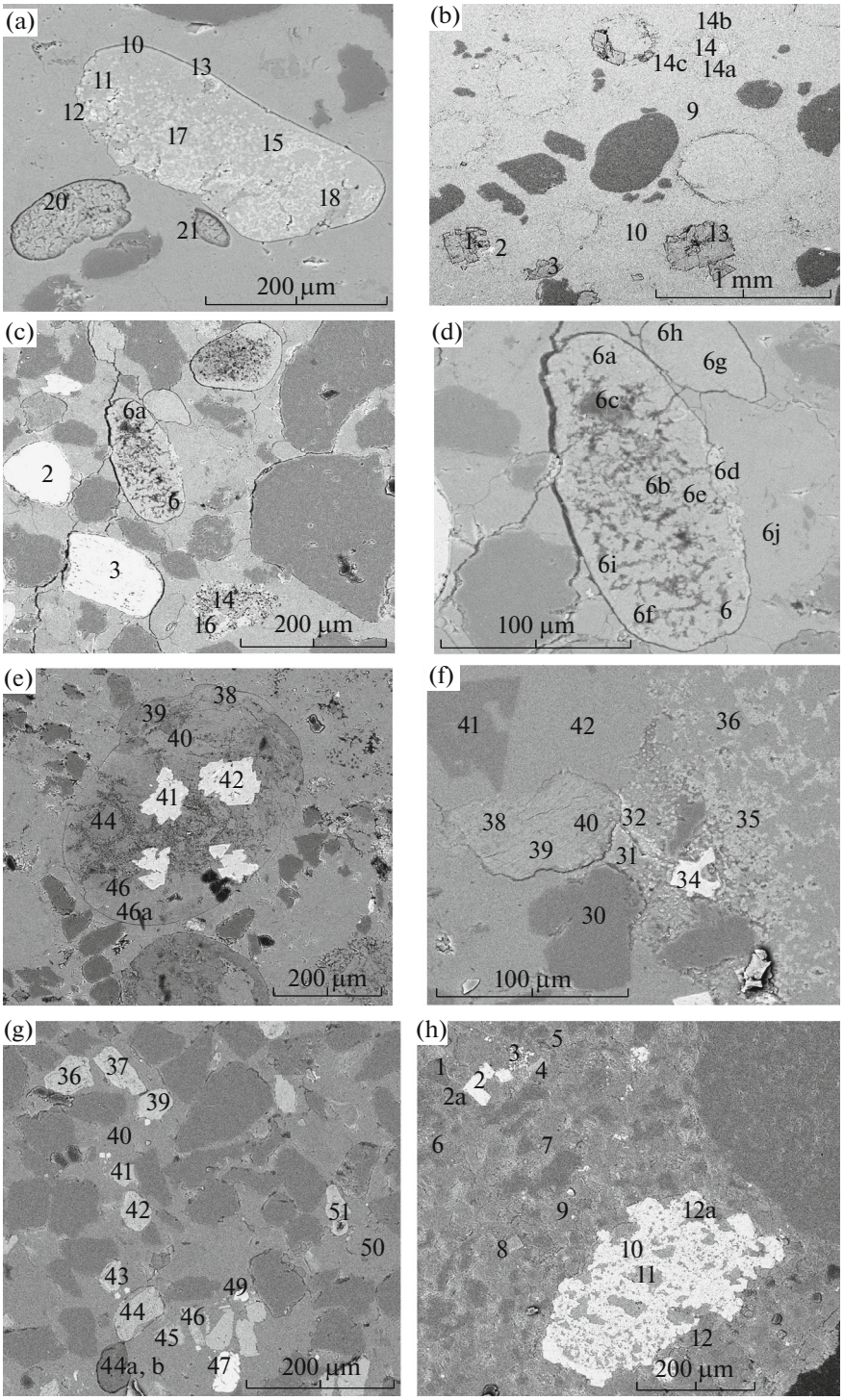

Fig. 5. Variably preserved glauconite grains in the terrigenous–carbonate rocks: (a–e, g) Chuskuna Formation (samples 607, 598, 606/4, 606/3, 596), (f) Erkeket Formation (sample 592). Polished thin section. SEM. (a, b) Glauconite grains in limestone with the admixture of quartz grains (hereinafter, dark gray is quartz) (sample 607): (a) (analyses 10, 15, 20, 21) glauconite, (an. 11) phosphate, (an. 17, 18) calcite, (an. 12) pyrite, (an. 13) hematite; (b) (an. 1, 3, 13) Fe-dolomite with calcite admixture, (an. 2) siderite, (an. 9, 10) calcite, (an. 14) glauconite, (an. 14a) glauconite with phosphate admixture, (an. 14b, 14q) calcite; (c) glauconite grains in detrital limestone: (an. 2, 3) ilmenite, (an. 6, 6a) glauconite, (an. 14) calcite, (an. 16) phosphate (sample 598); (d) fragment of polished thin section, sample 598, large magnification: (an. 6d, 6i, 6h, 6g) glauconite, (an. 6q) OM, (an. 6d) phosphate, (an. 6f, 6j) calcite; (e) glauconite grain in the detrital–oolithic limestone (sample 606/4): (an. 38, 39, 44, 46) glauconite, (an. 41, 42) hematite, (an. 46a) pyrite microcrystal; (f) detrital limestone with glauconite (sample 592): (an. 38, 39, 40) glauconite, (an. 34) ilmenite, (an. 41) dolomite, (an. 31, 36, 42) calcite, (an. 32, 35) phosphate; (g) silty calcareous sandstone (sample 606/3): (an. 44a, 44b) glauconite, (an. 41, 45) TiO_2 (rutile), (an. 36–38, 42, 43, 45, 51) ilmenite, (an. 47) xenotime, (an. 49) zircon, (an. 40, 50) calcite); (h) sandy silt (sample 596): (an. 1, 2a, 11, 12, 12a) glauconite, (an. 8) anatase, (an. 2, 3, 10) pyrite, (an. 7) calcite, (an. 6, 5, 9) Fe-dolomite with calcite admixture, (an. 4) phosphate.

Table 1. Compositions of the studied samples based on the X-ray and microprobe data

Ord. no.	Unit no.	Sample no.	Rock	Mineral components	
				main	subordinate
First section, Khorbusuonka River					
1	9	592	Detrital limestone with glauconite	Calcite	Quartz, Fsp, mica, chlorite, dolomite*, OM, ilmenite, pyrite, zircon, hem, goethite
2	9	592A	Clayey limestone	Calcite, apatite	Dolomite, mica, chlorite
3	8	594	Sandstone and limestone with ooliths and glauconite	Quartz, calcite	Fe-dolomite*, phosphate, ilmenite, rutile, hem
4	8	594A	Oolithic limestone and dolomite	Calcite, Fe-dolomite	Quartz
5	7	594D	Detrital limestone with ooliths	Calcite	Fe-dolomite*, quartz*, pyrite, hem, phosphate
6	5	594E	Gravelstone with glauconite	Quartz	Calcite, Fe-dolomite, hem, ilmenite
7	6	594E1	Limestone with oolith and glauconite	Calcite	Quartz, ilmenite, pyrite, phosphate, hem
8	6	594E2	Silty limestone	Calcite	Quartz, Fe-dolomite*, mica*, chlorite*, anatase
9	6	594E3	Dolomite	Fe-dolomite	Calcite, quartz, Fsp*, pyrite, zircon, hem, phosphate
10	5	596	Glauconite sandy siltstone	Quartz	Calcite*, Fe-dolomite*, Fsp, mica, chlorite, anatase pyrite***, phosphate
11	5	595	Glauconite sandstone	Quartz	Calcite, Fe-dolomite*, Fsp, phosphate, pyrite, hem, OM, rutile, mica, chlorite
12	4	604	Sandy gravelstone	Quartz	Fe-dolomite, hem, hem
13	4	604A	Sandstone with glauconite	Quartz	Anatase, Fsp, Fe-dolomite*
14	3	603	Glauconite sandy–clayey siltstone	Quartz	Fe-dolomite***, calcite*, chlorite, mica, ilmenite, rutile, pyrite, hem
15	3	603A	Glauconite silty calcareous sandstone	Quartz	Calcite, Fe-dolomite*, chlorite, mica, ilmenite, rutile, pyrite, hem
16	2	598	Glauconite detrital limestone	Calcite	Quartz, ilmenite, anatase, zircon, pyrite, phosphate, OM, rutile
17	2	597	Sandstone, limestone with glauconite	Quartz, Calcite	Fe-dolomite*, Fsp, anatase, ilmenite, rutile
18	2	599D	Clayey siltstone and sandstone with glauconite	Quartz	Calcite, Fe-dolomite, Fsp, chlorite, mica, phosphate*, anatase
19	1	599B	Gravelly sandstone	Quartz	Calcite, Fe-dolomite, Quartz
20	1	599	Glauconitic detrital–oolithic limestone	Calcite	Quartz, Fe-dolomite*, apatite, ilmenite, rutile, zircon, OM, hem
21	1	1175/32	Glauconitic limestone	Calcite	Quartz*, apatite, pyrite

Table 1. (Contd.)

Ord. no.	Unit no.	Sample no.	Rock	Mineral components	
				main	subordinate
Second section, Olenek River					
22	9	608E	Clayey limestone	Calcite	Quartz, Fsp, Fe-dolomite, chlorite > micas
23	9	608D	Organogenic–detrital limestone with glauconite	Calcite	Quartz, mica, chlorite
24	8	608C	Glauconitic detrital–oolithic limestone	Calcite	Quartz, Fe-dolomite*, apatite, ilmenite, zircon, rutile , siderite*, OM
25	5	607	Glauconitic detrital–oolithic limestone	Calcite	Quartz, Fe-dolomite, pyrite, ilmenite, siderite, monazite
26	5	607	Carbonate ooliths	Fe-dolomite	Calcite
27	3	606/4F	Clayey siltstone with glauconite	Quartz	Chlorite > micas, Fe-dolomite, Fsp, hem
28	2	606/4	Glauconitic detrital–oolithic limestone	Calcite	Quartz, Fe-dolomite*, Fsp, hem***, pyrite, apatite, ilmenite***, rutile***
29	2	606/5	Glauconitic detrital–oolithic limestone	Calcite	Quartz, phosphate, pyrite, hem
30	1	606/3A	Glauconite, silty oolithic sandstone	Quartz	Calcite***, Fe-dolomite, Fsp*, ilmenite, rutile, zircon, pyrite, hem, xenotime
31	1	606/3	Glauconitic sandy siltstone	Quartz	Fe-dolomite, Calcite, Fsp, ilmenite, rutile, zircon, hem
32	1	606A	Coarse-grained sandstone	Quartz	Calcite, phosphate*, mica*, chlorite*
Third section, Khary–Yallakh River					
33		1783	Glauconitic detrital limestone	Calcite	Fe-dolomite, hem***, ilmenite***

(***) High content of components, (*) trace contents (X-ray data). Abbreviations: (Fsp) feldspar, (OM) organic matter.

mosaic texture, and fine-grained sandstones and siltstones with numerous ore interbeds and (or) clay component.

The terrigenous–carbonate rocks are bedded (from coarse- to micro- and fine-grained varieties) and massive. The bedding is horizontal, wavy, cross, and wavy-cross. It is emphasized by different size and content of terrigenous grains, as well as different content and composition of carbonate, clay, and ore minerals, and others.

The **clay component** in 11 samples of diverse lithological composition is represented by dioctahedral micaceous minerals and trioctahedral chlorite (Table 1). In chlorite, the even-order intensity is higher than the odd-order one, which indicates an elevated content of Fe^{2+} cations in the mineral structure. Micaceous minerals in terms of unit cell parameter *b* (9.04–9.06 Å) are ascribed to dioctahedral Al–Fe varieties.

Thus, the studied terrigenous–carbonate rocks were subjected to the initial and deep catagenesis. This follows from the conformal–regeneration textures of sandstones and siltstones with insignificant content of the clayey and carbonate component, as well as typomorphic association of clay minerals (dioctahedral mica and trioctahedral chlorite), which is noted in the sandstones, siltstones, and limestones (Table 1).

Ore minerals. Rocks from the lower part of the section (units 1–3) contain numerous mafic interbeds consisting of ilmenite and, to lesser extent, rutile, anatase, leucoxene, zircon, and other minerals. These grains show not only layerwise, but also random distribution. They occur in both terrigenous and carbonate rocks of the studied formations (Table 1, Figs. 5c, 5f, 5g). The

highest amount of grains was found in the siltstone interbeds (samples 603, 606/3) and fine-grained sandstones (sample 603A, 597, 606/3A) (Fig. 5g), more rarely in limestones (samples 599, 599A, 606/4, 606/4B) (sections 1, 2, units 1–3). Siderite (sample 607, 608C), xenotime (sample 606/3A), and monazite (sample 607) were found as rare grains of different size (Figs. 5b, 5g).

Pyrite forms framboids, separate microcrystals, and their aggregates, as well as microinclusions in glauconite grains (Figs. 5a, 5e). Sometimes, it replaces them up to almost complete pseudomorphs (sample 596) (Fig. 5h). Hematite is widespread in the studied samples, replacing both cement and other minerals. In particular, it frequently develops after pyrite, ilmenite, and Fe-dolomite, as well as after glauconite grains to different extent (Figs. 3d, 3f, 4g, 5e). The base of the Erkeket Formation contains goethite, which also replaces glauconite grains that are most weathered at this stratigraphic level (samples 592, 608C).

Phosphates are represented by apatite group minerals (further termed apatite). Apatite in separate interbeds of terrigenous and carbonate rocks form thin interrupted rims (2–10 μm) around the terrigenous grains of quartz, ilmenite, and other minerals, as well as replaces glauconite grains and calcite (samples 592, 594, 594E1, 595, 598, 599, 1175/32, 607, and others) (Figs. 5a–5d). In addition, apatite in the rocks compose separate semirounded and rounded grains (0.1–0.4 mm), as well as fragments of shells together with calcite. In the limestones of the Erkeket Formation, apatite is also present as finely dispersed segregations of different shape and size (Fig. 5f).

Mineralogical Features of Glauconite Grains

Glauconite in the terrigenous–carbonate rocks was studied as grains of different size and shape and as cement mass. As mentioned, glauconite grains in ooliths in the first (units 1, 6–8) and second (1, 2, 5, 6, 8) sections frequently fill up the central part (nucleus) (Figs. 4a, 4b, 5b), while the finely dispersed glauconite fills up separate concentric layers in them. It replaces organic remains up to complete pseudomorphs (samples 592, 594, and others). Glauconite grains are randomly distributed in the rocks. More rarely, they emphasize the vague bedding. Their content in the rocks varies from <1–3 to 10–15%.

The **grain shape** is globular (rounded, oval, nodular, cerebriform, ellipsoidal, flattened, and others) and irregular (semiangular, angular, and others) shapes. Irregular, frequently intricate shape resulted from the interaction of globules with the surrounding carbonate minerals (calcite, more rarely, Fe-dolomite) and quartz, while angular grains are formed during rewashing of the glauconite-bearing sediment (Figs. 3–5). Grains in the Erkeket Formation have both cerebriform and irregular shape (samples 592, 608C, 1783) (Figs. 3g, 3h, 4d), while grains in sample 1175/32 have rounded, irregular, and intricate shape, which is related to the different degree of their roundness (Figs. 3a, 3b).

The **grain color** is green of different intensity (Figs. 3, 4). The inner part of grains is frequently lighter than the marginal dark green zone, which sometimes acquires greenish yellow color owing to the glauconite replacement by goethite (sample 592). The surface has even and (or) patchy dark to light green (to whitish) color, which is related to the replacement of glauconite globules by calcite (samples 598, 599, 607, and others) and almost complete glauconitization of limestone (sample 1175/32). The surface of grains is smooth and (or) rough, frequently split by fractures filled with different minerals (quartz, apatite, calcite, hematite, and others).

The **grain size** changes from <0.1 to 1.0 mm. Grains in samples 606/3A, 606/3B, and 606/4A–606/4D are >1 to 1.8 mm long, while grains in sample 1175/32 reach 3 mm. The following size fractions were studied in detail (mm): 1.0–0.4 (sample 1175/32), 0.63–0.4 (samples 592, 606/5), 0.63–0.315 (sample 595), 0.4–0.315 (sample 598), 0.4–0.2 (sample 607), and 0.315–0.2 (samples 594, 599). In the polished thin sections, we analyzed grains of the following size (mm): 0.4–0.2 (sample 608C), 0.6–0.06 (sample 606/4), 0.2–0.08 (sample 596), 0.07–0.05 (sample 606/3A), 0.25–0.15 (sample 594E1).

The **grain density** in samples 1175/32, 592, 1783, 607, and 595 varies, in general, from 2.5 to ≥2.9 g/cm^3. From the light to heavy fractions, the intensity of green color slightly increases. Grains with a density of ~2.9 and ≥2.9 g/cm^3 are characterized by the high apatite content (sample 1175/32, 607), as well as goethite admixture (sample 592: 0.63–0.4 mm, ~2.9 g/cm^3).

The grains usually have random internal structure caused by the chaotic arrangement of microcrystals. Homogenous grains are rare, while almost all samples contain mainly heterogeneous varieties. This heterogeneity is caused by structural features of grains, type of extinction, and mainly by the presence of inclusions of other minerals (pyrite, apatite, calcite, hematite, and others) and OM in their cores and (or) rims, as well as over the entire grain area (Figs. 3–5, 6).

The SEM study showed that the outer and inner surface of grains are made up of gently bending and variably oriented microcrystals (from 1–2, rarely up to 4 μm), which can be grouped in peculiar segregations (Figs. 6a–6d). Such pattern is typical of glauconite. In grains of sample 1175/32, glauconite occurs in some places as lamellar microcrystals and cryptocrystalline mass that partially or completely fills up large parallel plates in a mixture with calcite crystals (Fig. 6e). In other places, glauconite has a massive and spongy microstructure, frequently developed in a mixture with calcite and OM film against this background (Fig. 6f).

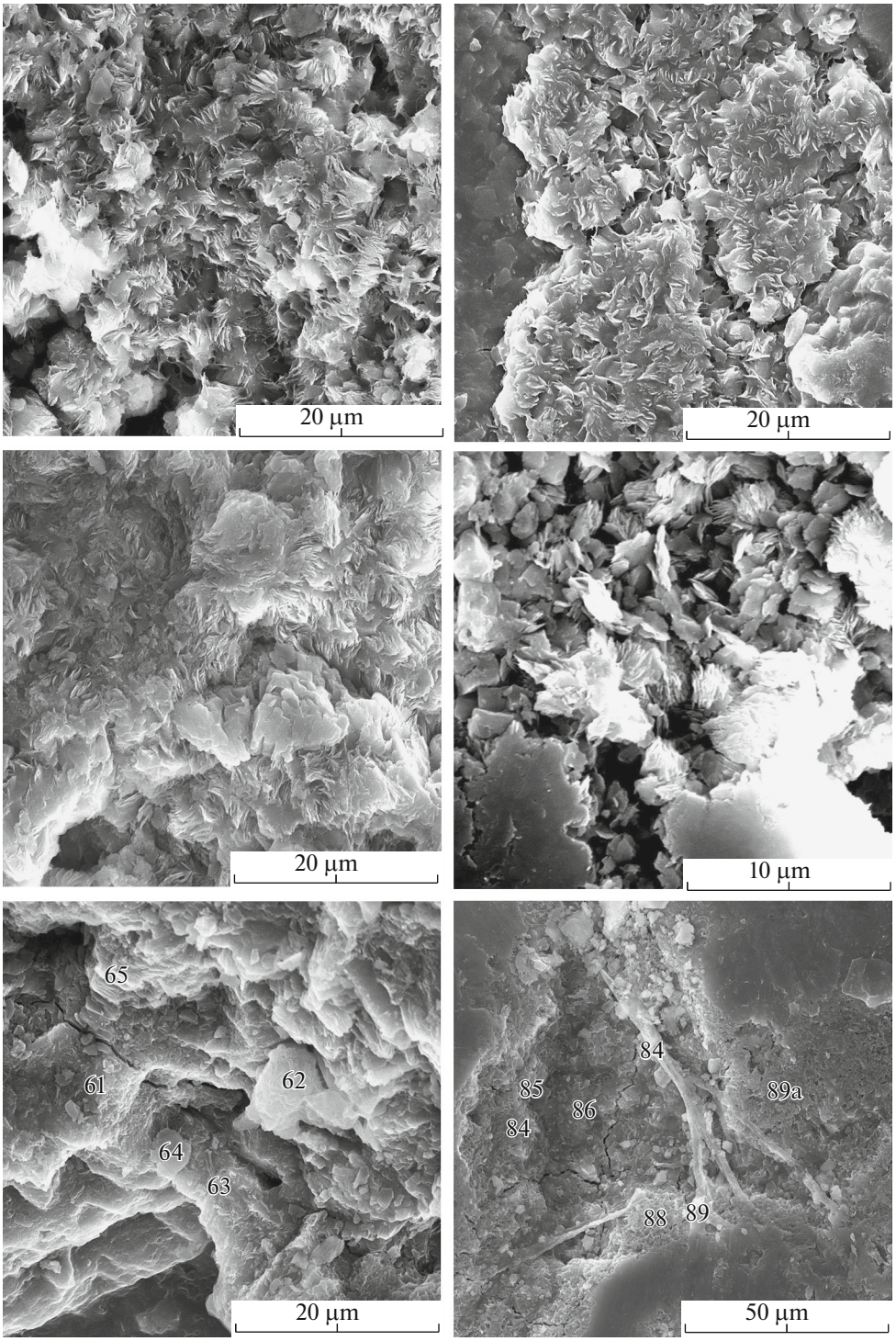

Fig. 6. Microtexture of glauconite in the studied grains (SEM). (a, b) Typical imbricated microtexture with thin microcrystals in the glauconite grains from sandstones and limestones (samples 595 and 606/4, respectively); (c, d) denser imbricated microtexture with isolated or grouped glauconite microcrystals from limestone (samples 599 and 607, respectively) (massive calcite crystals are located almost in the central part of sample 599); (e, f) limestone of sample 1175/32: (e) platy glauconite microcrystals (an. 62) and cryptocrystalline glauconite mass (an. 61, 63) partially or completely filling large parallel plates in a mixture with calcite crystals (an. 62, 64); (f) massive and spongy glauconite microtexture, sometimes in a mixture with calcite (1.45–2.56%) (an. 84–86, 88, 89a) with OM film against the background (an. 89).

X-Ray Data

Analysis of the XRD patterns recorded from the natural and ethylene glycol-saturated oriented specimens was carried out following the procedure in (Drits et al., 1993; Ivanovskaya et al., 2012). The studied samples consist of the mixed-layer mica–smectite aggregates with relatively low (≤10%) and higher (10–20%) contents of expandable layers (samples 594, 595, 598, 607 and samples 592, 599, 1175/32, 606/5, 1783, respectively). Sample 595 shows the traces of chlorite. Among non-clay minerals, other samples contain apatite and (or) calcite.

The mixed-layer phases are characterized by both disordered alternation of mica and smectite layers and tendency to ordering (short-range factor $R = 0$ and $R \geq 1$, respectively), which follows from different diffraction features of the ethylene glycol-saturated oriented specimens. In the first case, the XRD patterns show one reflection in the low-angle region, which is shifted toward higher angles θ. Its *d* values vary from 9.88 Å to 10.05 Å (samples 592, 594, 595, 598, 1175/32, 607, 606/5, and 1783). In the second case, the first low-angle reflection is split into two reflections with $d =$ 11.05 Å and $d = 9.72$ Å (sample 599).

Analysis of the XRD patterns of unoriented specimens of the studied samples allowed us to determine the close degree of structural ordering for two of them (samples 595, 11783). In particular, the XRD powder patterns of these samples show relatively low and wide reflections with $d = 3.642$, 3.647, and 3.069, 3.084 Å; weak reflection with $d \sim 4.34$ and 4.39 Å; and small bend in the region with $d \sim 4.12$ and 4.15 Å. Similar pattern is typical of samples with moderate ordering (Drits et al., 1993). In other studied samples, the admixture of calcite and other minerals (quartz, goethite, phosphate, and others) prevented the determination of degree of their crystallinity. The parameter *b* of the minerals varies from 9.06 to 9.12 Å (d (060) = 1.510–1.520 Å), which indicates their glauconite composition.

Cation Composition

The crystal-chemical formulas of dioctahedral layer silicates were calculated for the anion framework $O_{10}(OH)_2$ using the complete silicate microanalyses (samples 1783, 607, 1175/32), quantitative microprobe analysis (sample 595), and semiquantitative microprobe analyses (samples 592, 594, 608C, 594E1, 596, 606/4, 606/5, 598, 606/3A, 599), with allowance for the Mossbauer data (Tables 2, 3). The studied layer silicates show variations in the content of tri- and bivalent cations in the octahedral sheets of 2 : 1 layers: Al 0.94–0.16, Fe^{3+} 1.28–0.63, Fe^{2+} 0.33–0.13, Mg 0.37–0.22 f. u. (Table 3). Based on the isomorphic substitution of Fe^{3+} and Al^{3+} in octahedra, according to the IMA NC and AIPEA NC classifications (Rieder et al., 1998; Guggenheim et al., 2006) and the data in (Kossovskaya and Drits, 1971; Ivanovskaya et al., 2012, 2015, 2017; Zviagina et al., 2017), these silicates are subdivided into glauconite and Al-glauconite ($^{VI}Al/(^{VI}Al + {}^{VI}Fe^{3+}) = 0.11–0.47$ and 0.60, respectively) (Table 3, an. 1–11, 13, 14, and 12, respectively). Thus, in terms of the Al index, the studied micaceous minerals define a series from glauconite to Al-glauconite.

DISCUSSION

The Olenek Uplift in the Early Precambrian was located within the Yudoma–Olenek structural-facies region, large structural unit extending as a band (up to 500 km wide) along the northeastern margin of the Siberian Platform, which was covered by an open sea in the Early and Middle Cambrian (Kontorovich et al., 1999, Fig. 2). During the Early Precambrian, the Siberian Platform was occupied by an epicontinental basin (Rozanov and Khomentovsky, 2008; and others.). At the beginning of the Early Cambrian, the Siberian shallow-water epicontinental basin, including the studied territory, was a center of emergence and resettlement of main fauna groups (gastropods, hyoliths, brachiopods, and archeocyaths) (Missarzhevskii, 1980, 1982; Rozanov, 1980; Luchinina et al., 2013; and others). In particular, they were widespread in limestones forming in the warm shallow-water Erkeket basin (samples 592, 608C, 608D).

In the Chuskuna basin with the mixed terrigenous–carbonate sedimentation, numerous large faunal remains were found in individual limestone interbeds at close stratigraphic levels of both sections (samples 594B, 594D, 607C). Single skeletal remains were found in the calcareous sandstones (samples 594E1, 598A, 598, 606/4A, 606/3B). In the upper part of the Kessyusa Group (Formation), the terrigenous–carbonate rocks contain diverse small skeletal fossils (gastropods, hyoliths, hyolithelminths, and others) (Missarzhevsky, 1980, 1982; Karlova and Vodanyuk, 1985; Rogov et al., 2015; Nagovitsin et al., 2015; and others). These authors studied the carbonate–terrigenous sediments of the Kessyusa Group, but did not analyze the facies settings of their formation. The exception is the work by Marusin (2016), who ascribed the upper part of the Kessyusa Group to the lower part of the prefrontal beach zone and shelf–beach transitional zone with ichnofacies Cruziana based on the study of lithologies, bioturbations, and a complex of fossil traces of vital activity in the Kessyusa Group of the Olenek Uplift, in particular, in the Mattaia and Chuskuna formations in sections along the Khorbusuonka and Olenek rivers (Marusin, 2016, Fig. 4). According to the existing concepts (Reineck and Singh 1981; *Obstanovki ...*, 1993; and others), the settings of prefrontal beach zone in the facies profile of marine coast correspond to the wave disturbance zone, whereas transitional settings in the profile are located below the influence of common wave basis and correspond mainly to calm hydrodynamic conditions, which were

Table 2. Chemical composition of the studied Lower Cambrian samples (wt %)

Analysis no.	Sample no.	Grain no., mm	Grain density, g/cm^3	Oxides						
				SiO_2	Al_2O_3	Fe_2O_3	FeO	MgO	K_2O	Σ
Erkeket Formation										
1	592	0.63–0.4	~2.9	49.40	8.51	21.11	2.18	2.78	7.30	91.29
2	1783	0.63–0.2	2.6–2.7	48.44	9.12	19.81	2.05	2.90	7.77	90.36
Chuskuna Formation										
3	594	0.315–0.2	–	50.42	7.26	20.52	3.05	2.68	7.40	91.33
4	608C	0.4–0.2	–	49.83	7.11	18.98	4.44	2.79	7.39	90.53
5	594E1	0.25–0.15	–	49.70	6.69	20.57	3.05	2.98	6.98	89.98
6	607	0.4–0.2	2.7–2.9	47.35	5.71	21.96	5.14	2.66	6.80	90.30
7	596	0.2–0.08	–	50.91	9.84	16.11	2.39	3.32	7.23	89.80
8	595	0.63–0.315	2.5–2.9	51.03	10.20	18.20	2.70	3.27	8.54	94.00
9	606/4	0.6–0.05	–	51.48	7.82	17.26	4.04	2.74	7.19	90.53
10	606/5	0.63–0.4	–	49.50	7.11	19.61	4.59	2.56	7.22	90.58
11	598	0.4–0.315	–	49.16	8.31	20.91	3.10	2.40	8.31	92.18
12	606/3A	0.07–0.05	–	51.81	14.20	11.67	2.73	2.67	7.03	90.11
13	599	0.315–0.2	–	50.47	12.14	15.13	2.25	2.83	7.49	90.31
14	1175/32	1.0–0.4	≥2.9	47.46	5.56	21.84	4.26	1.88	7.15	88.85

Analyses are given excluding water. (An. 2, 6, 14) Complete silicate microanalysis after the subtraction of admixtures (C_{org}, $CaCO_3$, and $Ca_3(PO_4)_2$). Admixtures of calcites and phosphates in an. 2, 6, and 14 are, respectively, 3.36 and 0.37; 12.69 and 5.17; 26.04 and 7.98%. Total is given with allowance for contents of the following cations (%): samples 1783: Na_2O = 0.27; sample 607: CaO and Na_2O = 0.29 and 0.39, respectively; sample 1175/32: CaO and Na_2O = 0.30 and 0.40, respectively; sample 595: CaO = 0.02 (Camebax microprobe quantitative analysis). (An. 1, 3, 4, 5, 7, 9–13) semiquantitative microprobe analysis of the cation composition in separate grains. Analyses were calculated (1–14) using the Mossbauer data. Dash (hereinafter) means data are absent.

periodically disturbed by short-term storm events accompanied by the erosion of upper sediment beds and the redeposition of its components. Using these data, let us consider the stages of formation and transformation of glauconite grains.

Stages of the Formation and Transformation of Glauconite Grains

The Chuskuna shallow-water shelf was characterized by the mixed carbonate–terrigenous sedimentation (Fig. 2), which caused periodic changes of sedimentation (physicochemical parameters, tectonic mode). In particular, relatively calm conditions providing the glauconite formation in the early diagenesis zone alternated with the hydrodynamically active settings, which led to the decomposition and rewashing of the glauconite-bearing sediments and, likely, to the proximal transfer of grains over the paleobasin. During rewashing in the stirring zone, separate glauconite grains served as nuclei for the oolith formation. With a further change of sedimentation setting, separate glauconite grains, glauconite nucleii within ooliths, as well as nucleus-free ooliths, and ooliths with nucleii of another composition (quartz, calcite, and others) were mixed and buried in situ or transferred, being involved in the newly formed sediments as suballochthonous admixture.

The final phase of the early diagenetic stage of terrigenous–carbonate rocks of the Chuskuna Formation was characterized by the alternation of conditions with relatively calm sedimentation and increased hydrodynamic activity, which provided the accumulation of alternating sediments of different composition (limestones of different type, gravelstones, sandstones, siltstones, and mudstones). Calm sedimentation follows from the horizontal bedding of rocks, while mobile setting is confirmed by the cross- and cross-wavy bedding, the presence of pebble, gravel, and coarse-grained (frequently poorly rounded) material, as well as the enrichment of separate interbeds in ore minerals, rough bedding planes, accumulations of allothigenic glauconite grains and ooliths, fragments of fauna, and others.

Ooliths in the studied sequences are developed at different stratigraphic levels. However, they are mainly confined to limestones with variable content of terrigenous admixture and more rarely to calcareous limestones (samples 594C, 594D, 594E1, 599, 606/4, 606/5, 607, 607A–607C, 608A–608C and samples 594, 606/3A, respectively) (Fig. 2). The highest content of ooliths with glauconite nuclei is noted in lime-

Table 3. Crystal-chemical formulas of the studied samples

Analysis no.	Sample no.	Grain size, mm	Grain density, g/cm^3	Cations										K_{Al}	Charges			Fe^{2+}/Fe^{3+}
				tetrahedral		octahedral					interlayer				tetrahedral	octahedral	interlayer	
				Si	Al	Al	Fe^{3+}	Fe^{2+}	Mg	Σ_{oct}	K	Ca	Na					
Erkeket Formation																		
1	592	0.63–0.4	~2.9	3.66	0.34	0.41	1.18	0.14	0.31	2.05	0.69	–	–	0.26	15.66	5.64	0.69	0.12
2	1783	0.63–0.2	2.6–2.7	3.63	0.37	0.44	1.12	0.13	0.32	2.01	0.74	–	0.04	0.28	15.63	5.58	0.78	0.12
Chuskuna Formation																		
3	594	0.315–0.2	–	3.74	0.26	0.38	1.15	0.19	0.30	2.02	0.70	–	–	0.25	15.74	5.55	0.70	0.17
4	608C	0.4–0.2	–	3.75	0.25	0.38	1.07	0.28	0.31	2.04	0.71	–	–	0.26	15.75	5.54	0.71	0.26
5	594E1	0.25–0.15	–	3.75	0.25	0.34	1.17	0.19	0.34	2.04	0.67	–	–	0.23	15.75	5.58	0.67	0.17
6	607	0.4–0.2	2.7–2.9	3.65	0.35	0.16	1.27	0.33	0.31	2.07	0.67	0.02	0.06	0.11	15.65	5.58	0.77	0.26
7	596	0.2–0.08	–	3.76	0.24	0.62	0.90	0.15	0.37	2.02	0.68	–	–	0.41	15.76	5.56	0.68	0.17
8	595	0.63–0.315	2.5–2.8	3.66	0.34	0.52	0.98	0.16	0.35	2.01	0.78	0.00	–	0.35	15.66	5.55	0.79	0.17
9	606/4	0.6–0.05	–	3.82	0.18	0.50	0.96	0.25	0.30	2.01	0.68	–	–	0.34	15.82	5.50	0.68	0.26
10	606/5	0.63–0.4	–	3.73	0.27	0.36	1.11	0.29	0.29	2.05	0.69	–	–	0.25	15.73	5.58	0.69	0.26
11	598	0.4–0.315	–	3.65	0.35	0.38	1.17	0.19	0.27	2.01	0.79	–	–	0.24	15.65	5.56	0.79	0.17
12	606/3A	0.07–0.05	–	3.73	0.27	0.94	0.63	0.16	0.29	2.02	0.65	–	–	0.60	15.73	5.62	0.65	0.26
13	599	0.315–0.2	–	3.69	0.31	0.74	0.83	0.14	0.31	2.02	0.70	–	–	0.47	15.69	5.61	0.70	0.17
14	1175/32	1.0–0.4	≥2.9	3.70	0.30	0.21	1.28	0.28	0.22	1.99	0.71	0.02	0.06	0.14	15.70	5.48	0.81	0.22

(K_{Al}) Aluminum index $^{VI}Al/(^{VI}Fe^{3+} + {}^{VI}Al)$.

stones of the second section (samples 607, 607A, B) (Figs. 4a, 4b). In the majority of collected samples, glauconite grains of different shape (including globular ones) occur not only in rock, but also within ooliths, which indicates, as noted above, the redeposition of glauconite (Figs. 4a, 4b). Thus, allothigenic grains, as authigenic ones, can be characterized by regular shape (rounded, oval, ellipsoidal, and others), which was noted previously (Nikolaeva, 1977, and others). This complicates the interpretation of their genesis. It is known that convincing criteria of their genesis in sandy–silty rocks can be represented by the size proportions of terrigenous and glauconite grains. In particular, separate levels of the studied sections, in addition to small grains (0.05–0.2 mm), also comprise coarse (up to 1.0 mm) globules, the size of which exceeds that of quartz grains. Such pattern is observed in the bedded sandy siltstones (sample 596) and thin-bedded fine-grained silty sandstones (samples 606/3A, 606/3B). The last rocks comprise grains up to 1.3 mm, while the size of separate glauconite globules in the alternating siltstones and limestones varies from 1.0 to 1.8 mm (samples 597, 606/4A–606/4D), which together with their globular shape likely indicates their authigenic origin. Thus, separate samples of the Chuskuna rocks contain not only allothigenic glauconite, but also small amount of authigenic globules formed at the final stage of early diagenesis. They are coarser than quartz grains and (or) reach significant size and have a globular shape. Recall that the glauconite grains are soft material and easily subjected to abrasion.

Glauconite was formed during accumulation of the Mattaia and Chuskuna formations. In the diagenesis zone of initial (undisturbed) sediments, the authigenic glauconite was tightly associated with apatite and, likely, pyrite. In separate interbeds, apatite was developed after glauconite globules, while limestone was locally replaced by glauconite in the Mattaian time (sample 1175/32). The redeposited (allothigenic) glauconite grains again involved in the diagenesis zone and the newly formed glauconite are subjected to calcitization (more rarely, pyritization and phosphatization) (Figs. 3–6).

As mentioned above, the warm shallow-water Erkeket basin accumulated mainly organogenic limestones, which rest with erosion traces on the Chuskuna sandstones. The base of the Erkeket Formation comprises the redeposited grains and authigenic large globular (rounded, oval, cerebriform) grains (samples 592, 608C, 1783) (Figs. 3g, 3h, 4c, 4d), which were subjected to late calcitization and rarer phosphatization. It should be noted that high-Fe carbonate sediments transformed into limestones of the Erkeket Formation were unfavorable for the generation of glauconite. Correspondingly, the glauconite grains are present only at the base of the Erkeket Formation.

In the sandy–silty rocks subjected to deep catagenesis, separate glauconite grains could be deformed during gravity compaction and were replaced by quartz, as well as clay minerals, including chlorite, whose traces are noted in the globules (sample 595). It is possible that at this stage of transformations (or) slightly earlier, glauconite was replaced by Fe-dolomite (sample 594C), large crystals of which are also developed after calcite ooliths (Fig. 5b). In addition, calcite locally experiences partial recrystallization in the micritic limestone and the pore cement of sandstones. Recrystallization of the calcite could continue not only during catagenesis, but also during uplifting of the area at the stage of retrograde catagenesis. Modern supergene conditions resulted in the formation of hematite in the rocks and some glauconite grains (Figs. 3f, 4g, 5e).

Isotope-Geochronological Data

Preliminary Rb-Sr dating of four samples from the Erkeket (sample 1783), Chuskuna (samples 595, 607), and Mattaia (sample 1175/32) formations gave significantly rejuvenated dates (450–320 Ma), which do not correspond to the age value of 541.0 Ma previously accepted for the Vendian–Lower Cambrian boundaries (Gradstein et al., 2012). This can be related to diverse secondary alterations of glauconite, which proceeded at different diagenetic stages and spanned both authigenic and redeposited grains, as well as at the next stages of deep catagenesis and modern hypergenesis. Revealing the reasons of "rejuvenation" of the isotopic age of glauconites is the subject of further studies.

CONCLUSIONS

Glauconite is widely developed in the terrigenous–carbonate rocks of the upper Mattaia Formation and the lower Chuskuna Formation, as well as at the base of the Lower Cambrian Erkeket Formation (Tommotian Stage, zone *N. sunnaginicus*) on the northwestern slope of the Olenek Uplift.

Relatively calm conditions of marine sedimentation, which provided the formation of glauconite in the upper sediment layer, alternated with episodes of elevated hydrodynamic activity, resulting in the stirring and rewashing of glauconite-bearing sediments, and, sometimes, the formation of ooliths with nuclei consisting of morphologically diverse (including globular) glauconite grains extracted from primary sediments. During their subsequent burial, local microconditions in the diagenesis zone provided the formation of authigenic glauconite globule, which were associated with the allothigenic varieties. In some places, the authigenic glauconite makes up the cement in sediments and replaces organic remains up to the formation of complete pseudomorphs.

Our studies confirm the data on facies formation conditions of the Mattaia and Chuskuna sediments obtained by Marusin (2016) on the basis of macro-

scopic features of rocks, as well as bioturbations and traces of vital activity of fossils in the Kessyusa Group of the Olenek Uplift.

The most intense secondary alterations of the allothigenic and authigenic glauconite grains at different lithogenesis stages are calcitization, phosphatization, and ferrugination, as well as local pyritization of globules up to the formation of complete pyrite pseudomorphs, whereas the replacement of glauconite by Fe-dolomite and chlorite and the deformation of grains and their silicification are rarely observed.

The studied glauconite grains are represented by the mixed-layer mica–smectite phases with relatively low (<10%) or high (10–20%) contents of expandable layers. The micaceous minerals form a series from glauconite to Al-glauconite (Al index $K_{Al} = {}^{VI}Al/({}^{VI}Fe^{3+} + {}^{VI}Al)$ is 0.11–0.47 and 0.60, respectively), with the K_2O content varying from 6.80 to 8.54%. The mixed-layer phases are mainly represented by varieties with the disordered alternation of mica and smectite layers (the short-range factor $R = 0$), more rarely exhibiting ordering tendency ($R \geq 1$). The unit cell parameter b of the minerals varies from 9.06 to 9.12 Å.

In relation with intense secondary alterations, in spite of sufficiently high K content and relatively low content of smectite layers, the studied glauconite is not suitable for obtaining the stratigraphically significant age dates. Obtained Rb–Sr dates (450–320 Ma) reflect the age of later transformations of the sedimentary rocks and their deciphering is the subject of further studies.

FUNDING

This work was accomplished in accordance with the Research Program of the Geological Institute of the Russian Academy of Sciences (no. 0135-2016-0021). It was financially supported by the Russian Foundation for Basic Research (no. 17-05-00254) and the Presidium of the Russian Academy of Sciences (Program 17: project no. 0153-2018-0050, Program 19: project no. 0153-2018-0009).

ACKNOWLEDGMENTS

We are grateful to E.V. Shchepetova for constructive comments during the manuscript preparation.

REFERENCES

Drits, V.A. and Kossovskaya, A.G., Clay minerals: Micas and chlorites, in *Tr. GIN AN SSSR*, Moscow: Nauka, 1991, no. 465.

Drits, V.A., Kameneva, M.Yu., Sakharov, B.A., et al., *Problemy opredeleniya real'noi struktury glaukonitov i rodstvennykh tonkozernistykh fillosilikatov* (Problems in Determining the Real Structure of Glauconites and Cognate Fine-Grained Phyllosilicates), Novosibirsk: Nauka, 1993.

Geptner, A.R. and Ivanovskaya, T.A., Biochemogenic genesis of the glauconite–nontronite series minerals in present-day sediments of the Pacific Ocean, *Lithol. Miner. Resour.*, 1998, no. 6, pp. 503–517.

Gradstein, F.M., Ogg, J.G., Schmitz, M.D., and Ogg, G.M., *The Geologic Time Scale*, Elsevier, 2012, vol. 1.

Guggenheim, S., Adams, J.M., Bain, D.C., et al., Summary of recommendations of Nomenclature Committees relevant to clay mineralogy: report of the Association Internationale pour l'etude des Argiles (AIPEA) Nomenclature Committee for 2006, *Clays Clay Miner.*, 2006, vol. 54, pp. 761–772.

Ivanovskaya, T.A., Zaitseva, T.S., Zvyagina, B.B., and Sakharov, B.A., Crystal-chemical peculiarities of globular layer silicates of the glauconite–illite composition (Upper Proterozoic, Northern Siberia), *Lithol. Miner. Resour.*, 2012, no. 6, pp. 491–512.

Ivanovskaya, T.A., Zvyagina, B.B., Sakharov, B.A., et al., Globular layer silicates of the glauconite–illite composition in Upper Proterozoic and Lower Cambrian rocks, *Lithol. Miner. Resour.*, 2015, no. 6, pp. 452–477.

Ivanovskaya, T.A., Zvyagina, B.B., and Zaitseva, T.S., Secondary alterations of globular and platy phyllosilicates of the glauconite–illite series in the Precambrian and Vendian–Cambrian rocks, *Lithol. Miner. Resour.*, 2017a, no. 5, pp. 369–400.

Ivanovskaya, T.A., Zvyagina, B.B., and Zaitseva, T.S., Globular layer silicates of the glauconite–illite series in sediments of different lithological types and ages, in *Materialy Yubileinogo s"ezda Rossiiskogo mineralogicheskogo obshchestva "200 let RMO"* (Materials of the Jubilee Conference of the Russian Mineralogical Society "200 Years of RMO"), St. Petersburg, 2017b, pp. 220–222.

Karlova, G.A. and Vodanyuk, S.A., New data on the transitional-to-Precambrian sediments in the Khorbusuonka River basin (Olenek Uplift), in *Stratigrafiya pozdnego dokembriya i rannego paleozoya Sibiri. Vend i rifei* (Stratigraphy of the Late Precambrian and Early Paleozoic in Siberia: Vendian and Riphean), Novosibirsk: Nauka, 1985, pp. 3–13.

Knoll, A.N., Grotzinger, J.P., Kaufman, A.J., and Kolosov, P., Integrated approaches to terminal Proterozoic stratigraphy: an example from the Olenek Uplift, northeastern Siberia, *Precambrian Res.*, 1995, vol. 73, pp. 251–270.

Kontorovich, V.A., Gubin, I.A., Zoteev, V.V., et al., Structural-tectonic characteristics and model of the geological structure of Neoproterozoic–Phanerozoic rocks in the Anabar–Lena zone, *Geol. Geofiz.*, 2013, vol. 54, no. 8, pp. 1253–1274.

Kossovskaya, A.G. and Drits, V.A., Issues of the crystal-chemical and genetic classification of micaceous minerals in sedimentary rocks, in *Epigenez i ego mineral'nye indikatory* (Epigenesis and Its Mineral Indicators), Moscow: Nauka, 1971.

Luchinina, V.A., Korovnikov, I.V., Novozhilova, N.V., and Tokarev, D.A., Benthic Cambrian biofacies of the Siberian Platform (hyoliths, small shelly fossils, archeocyaths, trilobites and calcareous algae), *Stratigr. Geol. Correl*, 2013, vol. 21, no. 2, pp. 131–149.

Marusin, V.V., Fossil traces of the vital activity in Vendian/Cambrian boundary rocks on the Olenek Uplift, Sibe-

rian Platform, Abstracts of the PhD (Geol.–Miner.) dissertation, Novosibirsk: INGG SO RAN, 2016.

Missarzhevskii, V.V., Cambrian/Precambrian boundary beds on the western slope of the Olenek Uplift (Olenek River), *Byull. Mosk. O-va Ispyt. Prir., Otd. Geol.*, 1980, vol. 85, pp. 23–34.

Missarzhevskii, V.V., Subdivision and correlation of Precambrian/Cambrian boundary sequences based on some oldest groups of skeletal organisms, *Byull. Mosk. O-va Ispyt. Prir., Otd. Geol.*, 1982, vol. 57, no. 5, pp. 23–34.

Missarzhevskii, V.V., The oldest fossils and stratigraphy of Precambrian/Cambrian boundary sequences, in *Trudy GIN AN SSSR*, Moscow: Nauka, 1989, no. 443.

Nagovitsin, K.E., Rogov, V.I., Marusin, V.V., et al., Revised Neoproterozoic and Terreneuvian stratigraphy of the Lena–Anabar basin and north-western slope of the Olenek Uplift, Siberian Platform, *Precambrian Res.*, 2015, vol. 270, pp. 226–245.

Nikolaeva, I.V., *Mineraly gruppy glaukonita v osadochnykh formatsiyakh* (Minerals of the Glauconite Group in Sedimentary Formations), Novosibirsk: Nauka, 1977.

Reineck, H. E. and Singh, I. B., *Depositional Sedimentary Environments*, Berlin: Blackwell Sci. Publ., 1978. Translated under the title *Obstanovki terrigennogo osadkonakopleniya*, Moscow: Nedra, 1981.

Rieder, M., Cavazzini, G., D'yakonov, Y., et al., Nomenclature of the micas, *Can. Mineral.*, 1998, vol. 36, pp. 41–48.

Rogov, V.I., Karlova, G.A., Marusin, V.V., et al., Timing of the first Vendian biostratigraphic zone in the Siberian hypostratotype, *Geol. Geofiz.*, 2015, vol. 56, no. 4, pp. 735–747.

Rolli, M., Mouchet, P.O.J., and Kuebler, B., Determination and distinction of Ca-dolomites, Fe-dolomites, ankerite or stoichiometric dolomite by X-ray diffraction using a profile fitting, *Mem. Soc. Geol. France*, 1996, vol. 169, pp. 45–53.

Rozanov, A.Yu., Centers of the origin of Cambrian faunas, in *Mezhdunarodnyi geologicheskii kongress. 264-ya sessiya. Paleontologiya i stratigrafiya* (Int. Geol. Congress. 264 Session: Paleontology and Stratigrpahy), Moscow, 1980, pp. 30–34.

Rozanov, A.Yu., Khomentovskii, V.V., Shabanov, Yu.Ya., et al., To the problem of stage subdivision of the Lower Cambrian, *Stratigr. Geol. Correl*, 2008, vol. 16, no. 1, pp. 1–19.

Sedimentary Environments and Facies, Reading H. G., Ed., New York: Elsevier, 1986. Translated under the title *Obstanovki osadkonakopleniya i fatsii*, Moscow: Mir, 1990.

Vasil'ev, E.K. and Vasil'eva, N.P., *Rentgenograficheskii opredelitel' karbonatov* (The X-ray Handbook of Carbonates), Novosibirsk: Nauka, 1980.

Vodanyuk, S.A. and Karlova, G.A., The Kessyusa Formation in the Olenek Uplift, in *Pozdnii dokembrii i rannii paleozoi Sibiri. Rifei i vend* (Late Precambrian and Early Paleozoic in Siberia: Riphean and Vendian), Novosibirsk: Nauka, 1988, pp. 3–20.

Zaitseva, T.S., Semikhatov, M.A., Gorokhov, I.M., et al., Isotopic Geochronology and Biostratigraphy of Riphean Deposits of the Anabar Massif, North Siberia, *Stratigr. Geol. Correl.*, 2016, vol. 24, no. 6, pp. 549–574.

Zaitseva, T.S., Gorokhov, I.M., Semikhatov, M.A., et al., "Rejuvenated" globular phyllosilicates in the Riphean deposits of the Olenek Uplift (North Siberia): Structural identification and geological significance of Rb–Sr and K–Ar age data, *Stratigr. Geol. Correl.*, 2018, vol. 26, no. 6, pp. 611–633.

Zviagina, B.B., Drits, V.A., Sakharov, B.A., et al., Crystal-chemical regularities and identification criteria in Fe-bearing, K-dioctahedral 1M micas from X-ray diffraction and infrared spectroscopy data, *Clays Clay Miner.*, 2017, vol. 55, no. 4, pp. 234–251.

Translated by M. Bogina